E3S Web of Conferences **727**, 01005 (2026) https://doi.org/10.1051/e3sconf/202672701005
EEPES 2026

CFD-based optimization of a modified split-type reaction water turbine using response surface methodology

Murshied Aloyod[1,2*], and *Jaime* Honra[3]

[1]School of Graduate Studies, Mapua University, Manila, Philippines
[2]Mindanao State University – Sultan Naga Dimaporo, Lanao del Norte, Philippines
[3]School of Mechanical, Manufacturing, and Energy Engineering, Mapua University, Manila, Philippines

Abstract. This study addresses the need to improve the performance of split-type reaction water turbines (SRWTs) for low-head hydropower applications, where hydraulic losses and flow instability often limit torque output and efficiency. The objective was to optimize a modified SRWT by evaluating the effects of nozzle-edge sharpening angle, guide-pipe length, and guide-pipe diameter on torque and hydraulic efficiency. A CFD-based optimization framework was developed by integrating ANSYS Fluent simulations with Response Surface Methodology using a three-factor, three-level Box–Behnken Design. Fifteen design cases were simulated, and reduced quadratic models were established for torque and hydraulic efficiency, while pressure drop was analyzed as a supporting hydraulic indicator. Results showed that the sharpened nozzle angle had the strongest influence on both responses. The optimum design, consisting of a 52.02 mm guide-pipe length, 112.49 mm guide-pipe diameter, and 64.99° nozzle angle, produced a predicted torque of 31.22 N·m and hydraulic efficiency of 85.31%, which were closely confirmed by CFD. Compared with the baseline design, the optimized turbine improved torque by 41.42% and hydraulic efficiency by 41.44%. These findings demonstrate that CFD coupled with RSM is an effective tool for optimizing SRWT geometry for low-head hydropower applications.

1 Introduction

Global energy demand continues to increase, while fossil fuels remain dominant in the global energy mix, contributing to sustained carbon dioxide emissions and reinforcing the need for cleaner and more sustainable energy systems [1-2]. Among renewable energy technologies, hydropower remains one of the most mature, reliable, and widely implemented options. However, improving turbine performance under low-head and small-scale operating conditions remains a significant challenge, particularly for decentralized and rural energy applications. Split-type reaction water turbines (SRWTs) are attractive for such conditions because they can extract energy from both the pressure and kinetic components of flowing

* Corresponding author: mursh.thermo@gmail.com

water, making them suitable for low-head hydropower systems [3]. Despite this advantage, their performance is often restricted by internal flow instability and hydraulic losses, which reduce torque generation and overall turbine efficiency.

Previous studies have shown that SRWTs can be fabricated using low-cost and locally available materials, which strengthens their potential for rural electrification and off-grid deployment [4-5]. Experimental investigations reported efficiencies of approximately 65–70% under low-head conditions, while other studies demonstrated that rotor diameter, nozzle geometry, and flow-guiding modifications significantly affect turbine behaviour and performance [5-8]. Although these studies confirm the technical feasibility of SRWTs, many existing investigations focus only on isolated geometric modifications and do not comprehensively assess the combined effects of multiple design variables on turbine performance. As a result, the interaction among important geometric parameters remains insufficiently understood.

To address this gap, the present study develops a CFD-based optimization framework for a modified split-type reaction water turbine under low-head conditions. The study focuses on three geometric variables, namely nozzle-edge sharpening angle, guide-pipe length, and guide-pipe diameter, because these parameters are expected to directly influence flow guidance, internal momentum transfer, and energy conversion performance. The baseline and modified turbine configurations are illustrated in Figure 1. Using Computational Fluid Dynamics (CFD) and Response Surface Methodology (RSM) with a Box–Behnken Design (BBD), the study evaluates the effects of these geometric parameters on the primary performance responses, namely torque and hydraulic efficiency. In addition, pressure drop is included as a supporting response to examine its relationship with torque and hydraulic efficiency and to provide further insight into the hydraulic behavior of the turbine, although it is not treated as an optimization objective.

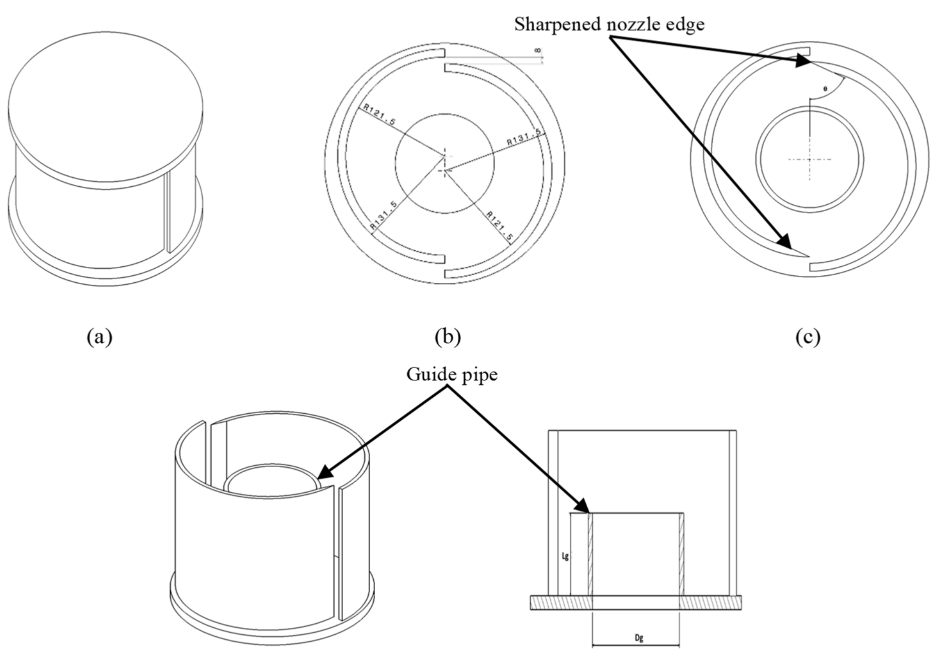

Fig. 1. Baseline design (a) isometric view, (b) top view open at the top and Modified SRWT geometry open at the top (c) top view, (d) isometric view and (e) section view.

2 Materials and Methods

2.1 Research framework

This study adopts a simulation-based optimization framework that combines CFD and RSM to improve the performance of a modified split-type reaction water turbine under low-head conditions. The overall methodological procedure, from geometry generation and CFD simulation to response surface modeling, optimization, and confirmation simulation, is summarized in Figure 2.

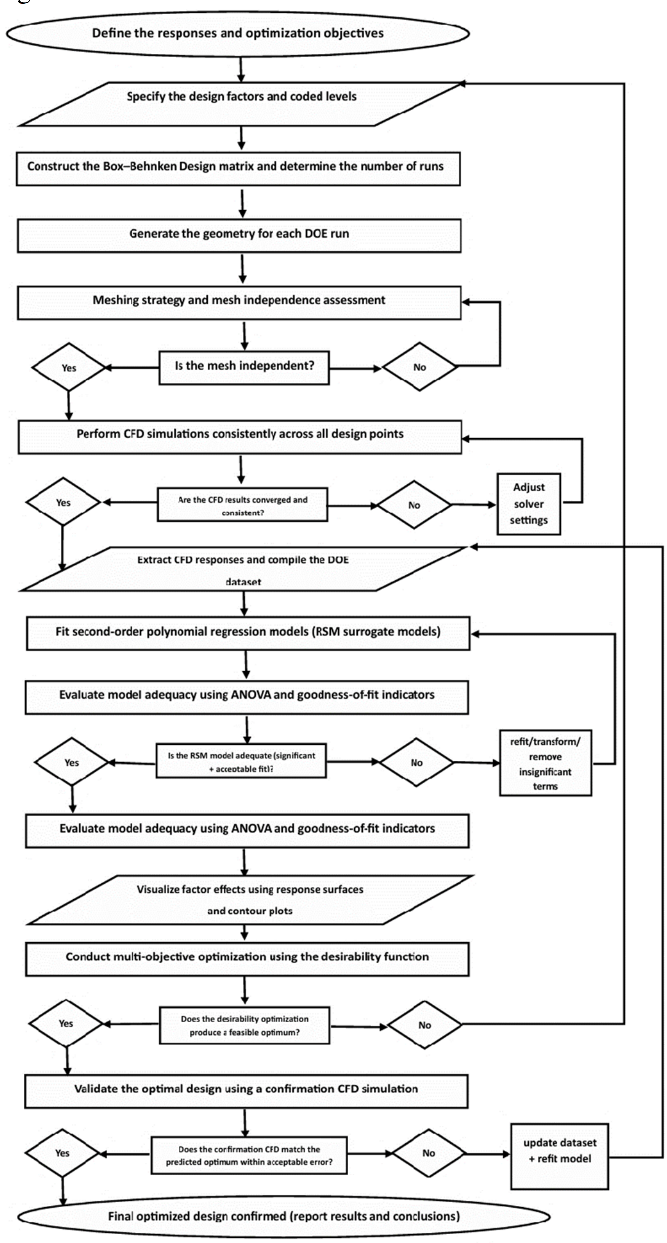

Fig. 2. CFD–RSM optimization workflow for the modified split-type reaction water turbine.

A Box–Behnken design was selected because it is an efficient response surface design for fitting second-order models, allowing the estimation of linear, interaction, and quadratic effects with fewer simulation runs than a full factorial design. This is particularly advantageous in CFD-based optimization, where each run is computationally expensive. Moreover, the design does not include points where all factors are simultaneously at their extreme levels, which helps avoid impractical geometries and promotes more stable numerical solutions [9].

2.2 Geometry and design variables

The baseline geometry used in the present study is adopted from the SRWT design of Date [6] and consists of a turbine diameter of 243 mm, a turbine height of 120 mm, a wall thickness of 10 mm, and a nozzle width of 8 mm. This configuration is used as the reference model for all comparisons. From this baseline, three geometric variables are selected for optimization: nozzle-edge sharpening angle (θ), guide-pipe length (Lg), and guide-pipe diameter (Dg). These variables are chosen because they directly influence flow development inside the turbine, particularly in the regions where the fluid is guided toward the exit and where hydraulic losses may become significant.

The nozzle-edge sharpening angle is varied at 25°, 45°, and 65°, while the guide-pipe length is assigned values of 48, 60, and 72 mm. Similarly, the guide-pipe diameter is varied at 97.2, 121.5, and 145.8 mm. These levels define a practical and numerically stable design space for the modified turbine geometry. The selected factor levels, together with the response variables considered in the study, are summarized in Table 1. In the present article, torque and hydraulic efficiency are treated as the primary optimization responses, whereas pressure drop is included as a supporting response for correlation and comparative analysis

Table 1. Design variables, factor levels, and response variables used in the study.

Factor/Response	Low (−1)	Center (0)	High (+1)	Role
A: Guide-pipe length (mm)	48	60	72	Independent variable
B: Guide-pipe diameter (mm)	97.2	121.5	145.8	Independent variable
C: Nozzle-edge angle (°)	25	45	65	Independent variable
Torque (N·m)	—	—	—	Primary response
Hydraulic efficiency (%)	—	—	—	Primary response
Pressure drop (Pa)	—	—	—	Supporting response

2.3 Design of Experiments

A three-factor, three-level Box–Behnken Design is employed within the RSM framework to generate the simulation matrix for the study. This design produces 15 simulation runs, including replicated center points that are useful for evaluating model adequacy and experimental error in the regression analysis. The design structure enables the development of second-order polynomial models for the selected primary responses while keeping the number of required CFD simulations manageable. The complete design matrix and the corresponding actual geometric values used in the CFD runs and responses are listed in Table

2. These 15 cases form the dataset used for subsequent response surface development and optimization.

Table 2. Design variables, factor levels, and response variables used in the study.

Run	A	B	C	Lg (mm)	Dg (mm)	θ (°)	Torque (N.m)	Hydraulic Efficiency (%)
1	+1	+1	0	72	145.8	45	27.53	75.35
2	−1	0	+1	48	121.5	65	31.21	85.31
3	0	−1	−1	60	97.2	25	24.39	66.64
4	0	0	0	60	121.5	45	27.75	75.84
5	−1	−1	0	48	97.2	45	27.60	75.42
6	0	0	0	60	121.5	45	27.75	75.85
7	−1	0	−1	48	121.5	25	24.42	66.73
8	0	−1	+1	60	97.2	65	31.17	85.18
9	0	+1	−1	60	145.8	25	24.42	66.83
10	+1	−1	0	72	97.2	45	27.62	75.46
11	0	0	0	60	121.5	45	27.63	75.58
12	+1	0	+1	72	121.5	65	31.06	84.88
13	−1	+1	0	48	145.8	45	27.55	75.40
14	0	+1	+1	60	145.8	65	30.99	84.82
15	+1	0	−1	72	121.5	25	24.45	66.83

2.4 CFD setup

All performance data were generated through CFD simulations carried out in ANSYS Fluent. The flow field was solved using the finite volume method within a Reynolds-Averaged Navier–Stokes framework. This numerical approach is suitable for the present work because it provides a practical balance between computational efficiency and predictive capability, which is necessary when multiple design cases are analyzed. The shear stress transport k–ω model, commonly referred to as the SST k–ω turbulence model, is a two-equation eddy-viscosity model that combines the near-wall accuracy of the k–ω model with the free-stream robustness of the k–ε model. In the present study, the SST k–ω turbulence model was selected because it is appropriate for internal flows involving separation and adverse pressure gradients [10], which are expected in the modified SRWT geometry.

In each design case, the main extracted responses are torque and hydraulic efficiency, which are used as the basis for response surface modeling and optimization. Pressure drop is also evaluated in each case to support the analysis of hydraulic loss behavior and to examine how it varies with the corresponding torque and efficiency values. However, pressure drop is not used as a target function in the optimization procedure.

2.5 Mesh generation

The computational domain is discretized using a predominantly unstructured tetrahedral mesh to accommodate the complex geometry of the modified split-type reaction water turbine. Local mesh refinement is applied in the guide-pipe and nozzle regions, where strong pressure and velocity gradients are expected, in order to improve the resolution of the internal flow field. In addition, inflation layers are generated along the solid walls to achieve better near-wall treatment and to support the requirements of the SST k–ω turbulence model. A representative view of the overall mesh distribution and the localized refinement in critical regions of the modified SRWT is presented in Figure 3.

To verify that the numerical results are not significantly affected by mesh density, a grid independence test is conducted using the principal performance parameters, namely torque and hydraulic efficiency, as summarized in Table 3.

Table 3. Design variables, factor levels, and response variables used in the study.

Mesh level	Number of elements	Torque (N·m)	Hydraulic efficiency (%)	Percent difference (%)
Coarse	1,053,895	21.42	58.55	—
Medium	2,185,483	21.60	59.04	0.85 / 0.84
Fine	3,865,400	22.08	60.34	2.20 / 2.19

Three mesh levels are examined and compared to evaluate the sensitivity of the computed responses to further mesh refinement. Based on the results, the fine mesh is selected for the final simulations because it provides the most resolved computational grid and yields the highest level of numerical accuracy. At the same time, the variations in the predicted torque and hydraulic efficiency relative to the coarser meshes remain within an acceptable range, indicating that the solution has reached mesh-independent behavior. Therefore, the fine mesh is adopted not only for the baseline case but also for all other simulation runs in the study to ensure consistency, accuracy, and reliability of the CFD results.

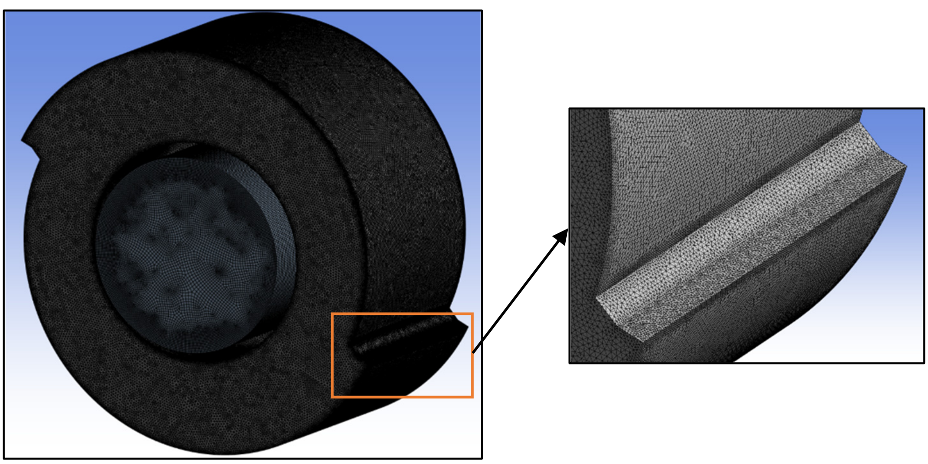

Fig. 3. Computational mesh of the modified SRWT showing global mesh distribution and local refinement in edges and nozzle regions.

2.6 Solver Settings and Boundary Conditions

The CFD simulations were conducted in ANSYS Fluent using a uniform numerical setup for the baseline turbine and all Box–Behnken design cases in order to ensure consistency and comparability of the computed results. A steady-state, pressure-based solver was employed, with the SIMPLE algorithm adopted for pressure–velocity coupling and second-order discretization schemes applied to the governing equations to improve numerical accuracy. The internal rotating flow was modeled using the Shear Stress Transport (SST) (k)–(\omega) turbulence model due to its suitability for resolving near-wall flow behavior and predicting adverse pressure-gradient effects in reaction water turbines. To represent the rotational motion of the turbine, the Multiple Reference Frame (MRF) approach was applied, with the rotating zone assigned a constant angular velocity of 200 rpm. For the boundary conditions, both velocity inlet and pressure inlet formulations were considered; however, the pressure inlet was selected as the primary inlet condition because it more appropriately represents the low-head, pressure-driven operating condition of the turbine. At the downstream boundary, a pressure outlet with 0 Pa gauge pressure was prescribed, while all solid surfaces were modeled as no-slip walls. The complete numerical settings and boundary-condition specifications adopted in the present study are summarized in Table 4.

Table 4. Design variables, factor levels, and response variables used in the study.

Category	Parameter	Setting / Value
Solver settings	CFD software	ANSYS Fluent
	Turbulence model	SST (k)–(omega)
	Application	Multiple Reference Frame
	Numerical setup	Same for baseline and all DOE cases
Boundary conditions	Velocity inlet option	2.11 m/s for Dg = 97.2 mm
		1.35 m/s for Dg = 121.5 mm
		0.936 m/s for Dg = 145.8 mm
	Primary inlet condition	Pressure inlet
	Inlet pressure	48,961.71 Pa
	Outlet condition	Pressure outlet, 0 Pa gauge
	Wall condition	No-slip, impermeable

2.7 Response surface modeling and optimization

The CFD results obtained from the 15 design runs listed in Table 2 are used to develop second-order response surface models for torque and hydraulic efficiency. The regression analysis is performed within the RSM framework, and Analysis of Variance (ANOVA) is applied to evaluate model significance, adequacy, and the contribution of the selected geometric parameters. Based on the fitted response surfaces, multi-response optimization is then carried out to determine the combination of nozzle-edge angle, guide-pipe length, and guide-pipe diameter that maximizes torque and hydraulic efficiency.

Although pressure drop is not treated as an optimization objective, it is included in the results analysis to examine its relationship with the two primary responses. In this way, pressure drop serves as a supporting hydraulic indicator that helps explain whether changes in turbine geometry associated with improved torque and efficiency are also accompanied by changes in hydraulic loss behavior. Finally, a confirmation CFD simulation is performed at the predicted optimum geometry to verify the reliability of the RSM predictions and to confirm the validity of the selected design.

3 Materials and Methods

3.1 CFD-Computed Performance Responses

The CFD-computed performance responses for the 15 Box–Behnken design runs are presented in Table 2. The table includes the coded and actual values of the geometric factors, namely guide-pipe length, guide-pipe diameter, and sharpened nozzle angle, together with the corresponding torque and hydraulic efficiency.

As shown in Table 2, the computed torque ranges from 24.39 to 31.21 N·m, while the hydraulic efficiency varies from 66.64% to 85.31%. Higher torque and efficiency were generally obtained at a nozzle angle of 65°, whereas lower values were associated with the 25° cases. The center-point runs also produced closely similar results, indicating good consistency of the CFD simulations.

These results confirm that the selected geometric parameters have a significant influence on turbine performance and provide the response dataset for the succeeding statistical analysis and optimization.

3.2 ANOVA and Model Summary for Torque and Hydraulic Efficiency

The statistical adequacy of the reduced quadratic models for torque and hydraulic efficiency is summarized in Table 5. Both models were highly significant, with model F-values of 8219.90 for torque and 8317.40 for hydraulic efficiency, and both had p-values less than 0.0001. These results indicate that the selected models adequately represented the response behavior within the studied design space.

As shown in Table 5, the torque model identified guide-pipe diameter (B), sharpened nozzle angle (C), the interaction terms AC and BC, and the quadratic terms A^2, B^2, and C^2 as significant. For hydraulic efficiency, the significant terms were C, AC, BC, A^2, B^2, and C^2. In both models, the sharpened nozzle angle was the most influential factor, indicating its dominant effect on turbine performance.

The lack-of-fit values in Table 5 were not significant for either response, with p-values of 0.9298 for torque and 0.9344 for hydraulic efficiency, confirming that both models fit the data well. In addition, the models showed excellent goodness of fit, with $R^2 = 0.9999$, adjusted $R^2 = 0.9998$, and predicted $R^2 = 0.9996$ for both responses. The high Adeq Precision values further indicate that the models provided a strong signal and were suitable for response surface analysis and optimization.

Table 5. Statistical adequacy of the reduced quadratic models for torque and hydraulic efficiency

Response	**Model F/P - values**	**Significant model terms**	**Lack-of-fit p-value**	**R^2**	**Adjusted R^2**	**Predicted R^2**	**Adeq Precision**
Torque	8219.90/ < 0.0001	B, C, AC, BC, A^2, B^2, C^2	0.9298	0.9999	0.9998	0.9996	238.1910
Hydraulic efficiency	8317.40/ < 0.0001	C, AC, BC, A^2, B^2, C^2	0.9344	0.9999	0.9998	0.9996	239.7899

3.3 Regression Equations of the Selected Models

After confirming the adequacy of the reduced quadratic models through ANOVA and diagnostic analysis, the fitted relationships for torque and hydraulic efficiency were expressed as regression equations. In response surface methodology, these equations describe the relationship between the design variables and the responses and are used for prediction within the studied design space. Design-Expert presents the models in both coded and actual forms; however, the actual-factor equations are emphasized in this study because they are more suitable for practical prediction using the original units of the variables.

3.3.1 Regression Equation for Torque

The final reduced quadratic model for torque in terms of actual factors is given by:

$$T=16.29287+0.050170A+0.042040B+0.166298C-0.000203AC-0.000110BC-0.000353A^2-0.000159B^2+0.000294C^2 \quad (1)$$

where A, B, and Cdenote guide pipe length, guide pipe diameter, and sharpened nozzle angle, respectively. The equation shows that torque was primarily influenced by the sharpened nozzle angle, with additional effects from interaction and quadratic terms, indicating a nonlinear response within the design space.

3.3.2 Regression Equation for Hydraulic Efficiency

The final reduced quadratic model for hydraulic efficiency in terms of actual factors is expressed as:

$$\eta=45.51277+0.127048A+0.096510B+0.452485C-0.000556AC-0.000282BC-0.000964A^2-0.000351B^2+0.000804C^2 \quad (2)$$

where A, B, and Crepresent guide pipe length, guide pipe diameter, and sharpened nozzle angle, respectively. Similar to the torque model, the efficiency equation indicates that sharpened nozzle angle had the strongest influence, while the interaction and quadratic terms confirm that the response surface was curved rather than purely linear.

3.4 Validation of the Developed Models

The adequacy of the developed regression models was assessed using the predicted-versus-actual plots for torque and hydraulic efficiency, as shown in Figure 4. These plots compare the CFD-computed response values with the corresponding values predicted by the fitted models. In both cases, the data points are closely distributed along the diagonal reference line, indicating a strong agreement between the numerical results and the model predictions. This pattern suggests that the fitted models are able to represent the response behavior within the selected experimental domain with good accuracy.

In Figure 4a, the predicted-versus-actual plot for torque shows that the data points closely follow the diagonal line, with only very small deviations. This indicates that the developed torque model provides reliable predictions of the CFD-computed values and captures the variation in torque across the design runs effectively. The close alignment of the points with the reference line also supports the adequacy of the model for response surface analysis.
Similarly, Figure 4b shows that the predicted hydraulic efficiency values are also in close agreement with the actual CFD-computed values. The points remain tightly clustered around

the diagonal line, indicating that the hydraulic efficiency model has acceptable predictive capability. The comparable behavior observed in both plots confirms that the developed models for torque and hydraulic efficiency are sufficiently accurate for subsequent statistical interpretation and optimization.

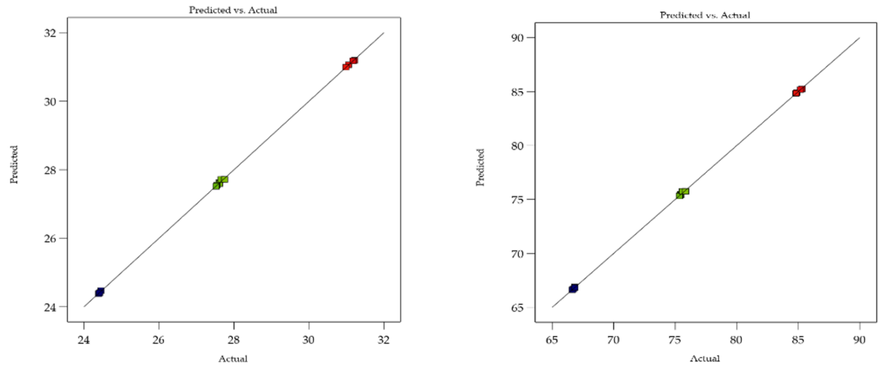

(a) (b)

Fig. 4. Predicted versus actual values for (a) torque and (b) hydraulic efficiency.

3.5 Response Surface Interpretation

Figure 5 presents the three-dimensional response surfaces for torque and hydraulic efficiency as functions of the selected geometric parameters. The plots show that both responses increased predominantly with increasing sharpened nozzle angle, indicating that this factor exerted the strongest influence on turbine performance. By contrast, guide pipe length and guide pipe diameter produced comparatively smaller effects and mainly acted as secondary variables that modified the response depending on their interaction with nozzle angle. This interpretation is consistent with the statistical analysis, which identified nozzle angle as the dominant term in both models.

For the torque response, Figure 5a shows that torque increased as the sharpened nozzle angle increased, while the effect of guide pipe length was less pronounced. Similarly, Figure 5b indicates that torque also improved with increasing nozzle angle, whereas guide pipe diameter exerted only a moderate modifying influence. For the hydraulic efficiency response, Figures 5 (c) and 5(d) exhibit the same general behavior, wherein efficiency increased markedly with increasing sharpened nozzle angle, while the effects of guide pipe length and guide pipe diameter remained secondary.

The visible curvature of the response surfaces further indicates that the relationships between the factors and the responses were not purely linear. This confirms the presence of interaction and quadratic effects in the fitted models. In general, the plots suggest that the most favorable region for both torque and hydraulic efficiency was located at higher sharpened nozzle angles combined with intermediate guide pipe dimensions. These graphical results therefore provide clear support for the adequacy of the reduced quadratic models and the location of the predicted optimum design.

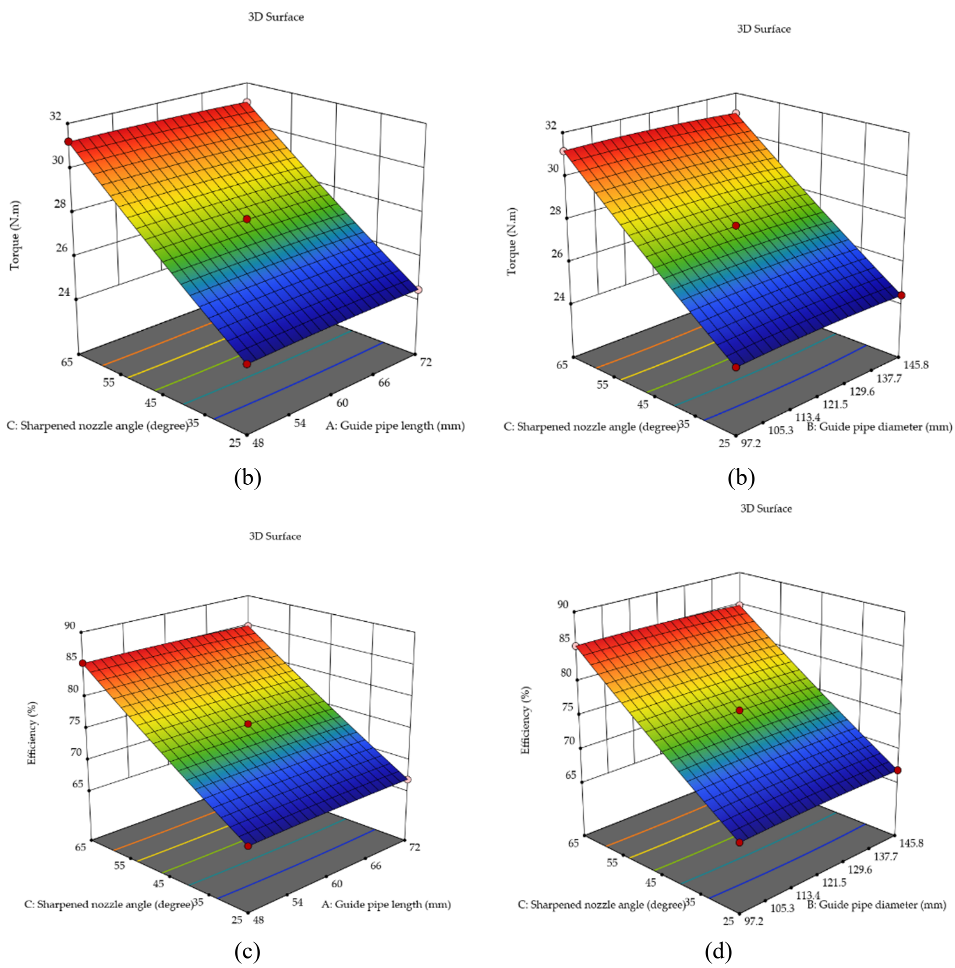

Fig. 5. 3D surface plot of Torque (a) Shaperned nozzle angle vs. Guide pipe length, (b) Shaperned nozzle angle vs. Guide pipe diameter, and 3D surface plot of Efficiency (c) Shaperned nozzle angle vs. Guide pipe length, (d) Shaperned nozzle angle vs. Guide pipe diameter.

3.6 Retionship of Pressure Drop with Torque and Hydraulic Efficiency

The relationship between pressure drop, torque, and hydraulic efficiency was examined using correlation analysis and scatter plots. As shown in Table 6, pressure drop had a very strong positive correlation with torque (($r = 0.993$)) and a strong positive correlation with hydraulic efficiency (($r = 0.885$)). This indicates that greater pressure drop across the turbine was generally associated with higher torque and improved efficiency. The trend suggests a more effective transfer of hydraulic energy to the runner, which enhanced the overall performance of the modified SRWT. A similar trend was reported by Sun et al. [11], where torque and pressure drop increased concurrently under changes in turbine parameters.

This trend is further illustrated in Figure 6(a), where torque increases almost linearly with pressure drop. The close clustering of the data points along the increasing trend suggests that pressure drop was a major hydraulic parameter governing torque generation. Similarly, Figure 6(b) shows that hydraulic efficiency also increased with pressure drop, although with slightly greater scatter than the torque relationship. This indicates that pressure drop remained a strong indicator of efficiency, but the association was somewhat less direct than for torque.

Table 6. Statistical adequacy of the reduced quadratic models for torque and hydraulic efficiency

Variable Pair	Correlation Coefficient, *r*	Interpretation
Pressure drop vs torque	0.993	Very strong positive correlation
Pressure drop vs hydraulic efficiency	0.885	Strong positive correlation

In general, the results suggest that an increase in pressure drop reflects greater hydraulic energy transfer within the turbine, leading to higher torque and improved hydraulic efficiency. Hence, pressure drop may be regarded as a reliable performance-related parameter for interpreting the hydraulic behavior of the modified SRWT.

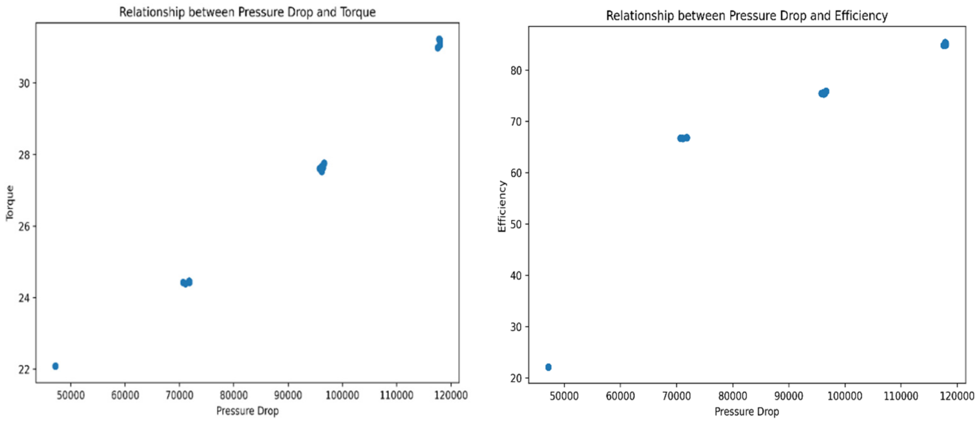

(a) (b)

Fig. 6. Scatter plots showing the relationship of pressure drop with (a) torque and (b) hydraulic efficiency.

3.7 Numerical Optimization

Numerical optimization was performed using the desirability function approach to determine the combination of guide-pipe length, guide-pipe diameter, and sharpened nozzle angle that simultaneously maximized torque and hydraulic efficiency. The optimization generated an optimum solution within the investigated design space, and this predicted design was subsequently verified through a confirmation CFD simulation. The predicted optimum geometry and the comparison between predicted and confirmed responses are presented in Table 7 and Table 8, respectively.

3.7.1 Optimum Solution from Desirability-Based Optimization

The desirability-based optimization identified the optimum geometry at a guide-pipe length of 52.02 mm, guide-pipe diameter of 112.49 mm, and sharpened nozzle angle of 64.9998°. At these settings, the developed models predicted a torque of 31.22 N·m and a hydraulic efficiency of 85.31%, with a desirability value of 1.000. This result indicates that the obtained factor combination is the most favorable numerical solution for achieving the defined optimization objectives.

3.7.2 Validation of the Optimum Design through Confirmation CFD Simulation

To verify the reliability of the predicted optimum solution, a confirmation CFD simulation was carried out using the optimized geometric parameters. The confirmation results show very close agreement with the model-predicted values, which indicates that the developed regression models have good predictive capability. As shown in Table 8, the difference between the predicted and CFD-confirmed values is very small for both responses. The torque prediction differs by only 0.0016 N·m, while the hydraulic efficiency differs by 0.0292%. The corresponding percentage errors are 0.0051% for torque and 0.0343% for hydraulic efficiency. These minimal deviations confirm that the desirability-based optimization and the developed response surface models are sufficiently accurate for predicting the optimum performance of the modified split-type reaction water turbine.

Table 7. Predicted optimum geometry and model-predicted performance responses.

Parameter	Predicted optimum value
Guide-pipe length, *Lg* (mm)	52.02
Guide-pipe diameter, *Dg* (mm)	112.49
Sharpened nozzle angle, θ (°)	64.99
Predicted torque (N·m)	31.22
Predicted hydraulic efficiency (%)	85.31
Desirability	1.000

Table 8. Predicted optimum geometry and model-predicted performance responses.

Response	Model-predicted	Confirmation CFD	Absolute difference	Percentage error (%)
Torque (N·m)	31.22	31.22	0.0016	0.0051
Hydraulic efficiency (%)	85.31	85.34	0.0292	0.0343

3.8 Baseline versus Optimized Design Performance

A comparison of the baseline and optimized designs is presented in Table 9. The optimized geometry produced higher torque and hydraulic efficiency than the baseline configuration, indicating improved turbine performance.

Table 9. Comparison of baseline and optimized turbine performance

Design	Torque (N·m)	Hydraulic efficiency (%)	Torque increase (%)	Efficiency increase (%)
Baseline	22.08	60.34	—	—
Optimized	31.22	85.34	41.42	41.44

The torque increased from 22.08 N·m to 31.22 N·m, corresponding to a 41.42% improvement. Likewise, the hydraulic efficiency increased from 60.34% to 85.34%, equivalent to a 41.44% increase. These results confirm that the optimized design provided a substantial enhancement in both output and energy conversion performance.

4 Conclusion

This study developed a CFD-based optimization framework for a modified split-type reaction water turbine operating under low-head conditions, with the aim of improving torque and hydraulic efficiency through variation of the nozzle-edge sharpening angle, guide-pipe length, and guide-pipe diameter.

The CFD results and response surface analysis confirmed that the selected geometric parameters significantly influenced turbine performance, with the sharpened nozzle angle emerging as the most dominant factor for both torque and hydraulic efficiency. The developed reduced quadratic models showed excellent statistical adequacy and predictive capability, while the response surfaces identified a favorable design region at higher nozzle angles combined with intermediate guide-pipe dimensions. Pressure drop also showed a very strong positive correlation with torque and a strong positive correlation with hydraulic efficiency, indicating that it is a useful supporting hydraulic indicator for interpreting turbine performance.

The desirability-based optimization predicted an optimum geometry of 52.02 mm guide-pipe length, 112.49 mm guide-pipe diameter, and 64.99° nozzle angle, corresponding to a predicted torque of 31.22 N·m and hydraulic efficiency of 85.31%. These predictions were closely validated by the confirmation CFD simulation, with only minimal percentage errors. Compared with the baseline design, the optimized turbine achieved a 41.42% increase in torque and a 41.44% increase in hydraulic efficiency, demonstrating the effectiveness of the proposed optimization approach. These findings contribute to the development of low-head hydropower systems by showing that CFD integrated with RSM can serve as a reliable and efficient tool for turbine geometry optimization while reducing dependence on costly experimental trial-and-error. From a practical perspective, the results provide useful design guidance for improving compact and potentially low-cost turbines intended for decentralized and rural energy applications. It is therefore recommended that future turbine design for low-head applications give particular attention to nozzle-edge angle, guide-pipe length, and guide-pipe diameter during the early design stage. Further work is also recommended to include experimental validation, wider operating-condition assessment, and additional geometric refinements in order to strengthen the real-world applicability of the optimized SRWT design.

The authors gratefully acknowledge the financial support provided by the Department of Science and Technology – Engineering Research and Development for Technology (DOST-ERDT). This support has been instrumental in the completion of this study and is sincerely appreciated.

References

1. Statistical Review of World Energy 2025, 74th ed. [Online]. Available: https://www.energyinst.org/statistical-review
2. "Global Energy Review 2025," 2025, [Online]. Available: https://www.iea.org/reports/global-energy-review-2025
3. A. Date, A. Date, A. Akbarzadeh, and F. Alam, "Examining the potential of split reaction water turbine for ultra-low head hydro resources," Procedia Eng., **49**, 197–204 (2012). https://doi.org/10.1016/j.proeng.2012.10.128

4. A. Date and A. Akbarzadeh, “Design and cost analysis of low head simple reaction hydro turbine for remote area power supply,” Renew. Energy, **34**, 409–415 (2009). https://doi.org/10.1016/j.renene.2008.05.012
5. A. Date and A. Akbarzadeh, “Design and analysis of a split reaction water turbine,” Renew. Energy, **35**, 1947–1955 (2010). https://doi.org/10.1016/j.renene.2010.01.023
6. A. Date, A. Date, and A. Akbarzadeh, “Performance investigation of a simple reaction water turbine for power generation from low head micro hydro resources,” Smart Grid Renew. Energy, **3**, 239–245, (2012). https://doi.org/10.4236/sgre.2012.33033
7. D. H. Allen and E. P. Villanueva, “A study on the performance of the split reaction water turbine with guide ribs,” IOP Conf. Ser. Mater. Sci. Eng., **88**, 012069 (2015). https://doi.org/10.1088/1757-899X/88/1/012069
8. G. C. H. Compasan and S. A. Guirnaldo, “Optimization of split reaction water turbine with guide cone using genetic algorithm,” Sci.Int. (Lahore), **35**, 469–473 (2023)
9. A. Witek-Krowiak, K. Chojnacka, D. Podstawczyk, A. Dawiec, and K. Bubała, “Application of response surface methodology and artificial neural network methods in modelling and optimization of biosorption process,” Bioresour. Technol., **160**, 150–160 (2014). https://doi.org/10.1016/j.biortech.2014.01.021
10. N. A. C. Sidik, S. N. A. Yusuf, Y. Asako, S. B. Mohamed, and W. M. A. A. Japa, “A short review on RANS turbulence models,” CFD Lett., **12**, 83–96 (2020). https://doi.org/10.37934/cfdl.12.11.8396
11. X. Sun, Y. Tan, X. Li, C. Ding, and Q. Hu, “The effect of downhole turbine modeling parameters on mechanical output performance,” Processes, **13**, 507 (2025). https://doi.org/10.3390/pr13020507